nature neuroscience

KCNQ4 K^+ channels tune mechanoreceptors for normal touch sensation in mouse and man

Matthias Heidenreich[1,2,9], Stefan G Lechner[2,9], Vitya Vardanyan[1,2,8], Christiane Wetzel[2], Cor W Cremers[3], Els M De Leenheer[4], Gracia Aránguez[5], Miguel Ángel Moreno-Pelayo[6], Thomas J Jentsch[1,2,7] & Gary R Lewin[2,7]

Mutations inactivating the potassium channel KCNQ4 (K_v7.4) lead to deafness in humans and mice. In addition to its expression in mechanosensitive hair cells of the inner ear, KCNQ4 is found in the auditory pathway and in trigeminal nuclei that convey somatosensory information. We have now detected KCNQ4 in the peripheral nerve endings of cutaneous rapidly adapting hair follicle and Meissner corpuscle mechanoreceptors from mice and humans. Electrophysiological recordings from single afferents from *Kcnq4*$^{-/-}$ mice and mice carrying a *KCNQ4* mutation found in DFNA2-type monogenic dominant human hearing loss showed elevated mechanosensitivity and altered frequency response of rapidly adapting, but not of slowly adapting nor of D-hair, mechanoreceptor neurons. Human subjects from independent DFNA2 pedigrees outperformed age-matched control subjects when tested for vibrotactile acuity at low frequencies. This work describes a gene mutation that modulates touch sensitivity in mice and humans and establishes KCNQ4 as a specific molecular marker for rapidly adapting Meissner and a subset of hair follicle afferents.

Our skin is richly innervated by mechanosensitive sensory fibers originating from the trigeminal and dorsal root ganglia (DRG). The most sensitive sensory afferents, called mechanoreceptors, have large, thickly myelinated axons and underpin our sensation of touch. Cutaneous mechanoreceptors do not represent a uniform population, but rather different mechanoreceptor types are functionally specialized to detect and encode different aspects of touch. For example, different mechanoreceptors are tuned to detect different qualities of touch, such as vibration, static indentation or stretch[1,2]. This modality specificity depends on the stimulus–response relationship and coding properties of the receptor and has been partly attributed to the mechanical properties of the so-called end organ[3,4]. Mechanoreceptors can encode the roughness of surfaces by acting as edge detectors that fire spikes at each surface irregularity as the fingertip is scanned across a surface[1,5,6]. Scanning textured surfaces is thus analogous to confronting mechanoreceptors with a complex vibration the frequency components of which are determined by the scan speed and the surface texture[7]. Notably, different types of mechanoreceptor have a characteristic tuning to certain frequency ranges that are likely to function in their ability to encode texture. The tuning of specific mechanoreceptors to certain types of mechanical stimulation must also be determined by the specific combination of voltage-gated ion channels a given mechanoreceptor expresses. The identity of such channels is likely to shed light on the mechanisms by which mechanoreceptor neurons are tuned to different frequency ranges.

KCNQ (Kv7) proteins form a distinct branch of the large Kv gene family of tetrameric K^+ channels[8]. KCNQ2 and KCNQ3 are almost exclusively found in neurons[9], whereas KCNQ4 and KCNQ5 are found in neurons[10–13] as well as in other tissues such as smooth and skeletal muscle[13,14]. KCNQ2–5 show properties of M currents, K^+ currents that are already partially open at resting potentials of neurons and that are highly regulated by G protein–coupled receptors including muscarinic acetylcholine receptors[15–17]. Their role in regulating neuronal excitability is best exemplified through the study of KCNQ2 and KCNQ3 mutations, which lead to benign familial neonatal convulsions in humans[9,18]. Loss of KCNQ2 function impairs neuronal spike-frequency adaptation and leads to epilepsy in mice also[19,20]. Moreover, immunocytochemistry analysis shows that KCNQ2, KCNQ3 and KCNQ5 are expressed in DRG neurons[21], where they may modulate pain sensitivity[22].

KCNQ4 is mutated in humans with DFNA2, a slowly progressing, autosomal dominant form of human hearing loss[12]. KCNQ4 is expressed in mechanosensitive cochlear outer hair cells[10,12], where it contributes to their resting membrane potential[23]. Loss of KCNQ4 function impairs hearing by interfering with the electromotility of sensory outer hair cells and, most importantly, by causing their progressive degeneration[23]. The expression of KCNQ4 in the CNS is restricted to certain structures in the brainstem, most notably to nuclei and tracts of the central auditory pathway and to trigeminal ganglia[10]. The role of trigeminal neurons in somatosensation prompted us to

[1]Leibniz-Institut für Molekulare Pharmakologie (FMP), Berlin, Germany. [2]Max-Delbrück-Centrum für Molekulare Medizin (MDC), Berlin, Germany. [3]Radboud University Nijmegen Medical Centre, Nijmegen, The Netherlands. [4]Department of Otorhinolaryngology, Head and Neck Surgery, Ghent University Hospital & Ghent University, Ghent, Belgium. [5]Servicio de Otorrinolaringología, Hospital General Universitario Gregorio Marañón, Madrid, Spain. [6]Unidad de Genética Molecular, Hospital Ramón y Cajal, IRYCIS, CIBERER, Madrid, Spain. [7]Cluster of Excellence NeuroCure, Charité-Universitätsmedizin Berlin, Berlin, Germany. [8]Present address: Institute of Molecular Biology, Yerevan, Armenia. [9]These authors contributed equally to this work. Correspondence should be addressed to T.J.J. (jentsch@fmp-berlin.de) or G.R.L. (glewin@mdc-berlin.de).

Received 30 August; accepted 11 October; published online 20 November 2011; doi:10.1038/nn.2985

investigate whether KCNQ4 is also present in sensory neurons of the DRG. Indeed, we found KCNQ4 in a small subset of DRG neurons and show that these represent two subtypes of rapidly adapting, low-threshold mechanoreceptors (RAMs). In the periphery, KCNQ4 channels are expressed in lanceolate endings and circular nerve fibers of hair follicles and in Meissner bodies, at sites where they can modulate stimulus–excitation coupling. In people with DFNA2, loss of KCNQ4 function increases their sensitivity to low-frequency vibration, and in mice, KCNQ4 mutations disrupt proper tuning of the mechanoreceptor response. Thus KCNQ4 modulates mechanosensitivity both in the cochlea and in the cutaneous sensory system, resulting in deafness and increased touch sensitivity, respectively.

RESULTS

KCNQ4 is expressed in a subset of mechanoreceptors

As KCNQ4 is present in neurons of somatosensory trigeminal ganglia in the brainstem[10], we asked whether it might also be found in DRG neurons that subserve body tactile sensation. Immunohistochemistry (IHC) for KCNQ4 in DRG sections showed specific labeling of approximately 10% of DRG neurons from *Kcnq4*$^{+/+}$ mice (**Fig. 1a**), but we observed no labeling in tissue sections from *Kcnq4*$^{-/-}$ mice (**Fig. 1b**). KCNQ4 protein was detected both at the plasma membrane and in intracellular puncta that are probably vesicular in nature (**Supplementary Fig. 1b**). All KCNQ4-positive DRG neurons were myelinated, as indicated by staining for neurofilament 200 (NF200) (**Fig. 1a**), and had medium to large cell size (810.6 ± 23.1 μm^2, s.e.m.; n = 131, **Supplementary Fig. 1a**). KCNQ4-positive neurons expressed neither nociceptor markers such as vanilloid receptor TRPV1 or the NGF receptor TrkA (data not shown), nor the proprioceptor marker parvalbumin (**Fig. 1c**), suggesting that they may represent low-threshold mechanoreceptors (LTMs). We next co-stained sections for KCNQ4 and either the receptor tyrosine kinase c-Ret or the transcription factor MafA, which have both been reported to be specific LTM markers[24,25]. Indeed, all KCNQ4-expressing neurons were immunopositive for c-Ret and most were MafA positive (**Fig. 1d,e**). MafA-positive neurons in the spinal cord[24], however did not stain for KCNQ4 (**Supplementary Fig. 2**). Moreover, KCNQ4-positive neurons could be back-labeled from the skin using a retrograde tracer (Alexa Fluor 488–coupled dextran) (**Fig. 1f**), suggesting that they are cutaneous mechanoreceptors.

KCNQ4 could be detected in the sensory endings of a subset of RAMs (**Fig. 2**), namely lanceolate and circular nerve endings around hair follicles (**Fig. 2a**), as well as in Meissner corpuscles in glabrous (non-hairy) skin (**Fig. 2c**), but was absent from *Kcnq4*$^{-/-}$ tissue (**Fig. 2b** and **Supplementary Fig. 3a,b**). We visualized sensory endings in the skin using double immunostaining with antibodies specific for NF200 or the calcium-binding protein S100b. Notably, consistent with KCNQ4 expression in trigeminal ganglion neurons[10], we also saw prominent KCNQ4 labeling at nerve endings surrounding sinus hairs of whisker pads (**Supplementary Fig. 3c**). In the glabrous skin of the footpads, Merkel cell–neurite complexes represent slowly adapting mechanoreceptors (SAMs)[1]. We did not detect KCNQ4 protein in Merkel cells, nor in their associated nerve fibers (**Fig. 2e**).

KCNQ4 was not detected in Pacinian corpuscle endings (**Fig. 2d**), another type of RAM best tuned to frequencies above 100 Hz (ref. 26). In this case we used sections of the interosseous membrane, which is enriched for these corpuscles. These results were obtained with two different antibodies, both of which detected KCNQ4 in skin and cochlear hair cells[10] in parallel control experiments (data not shown). We conclude that KCNQ4 is present in a subset of RAMs, where it is targeted to the peripheral endings where mechanical stimuli are transformed into action potentials.

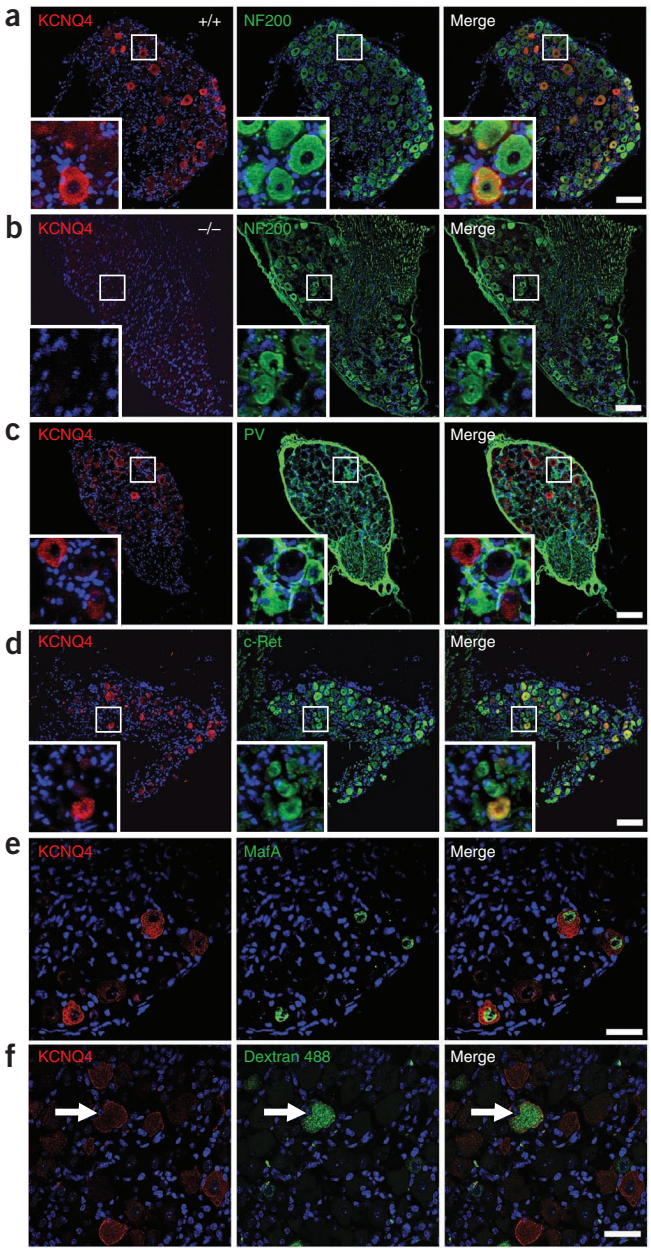

Figure 1 KCNQ4 is expressed in a subset of DRG neurons. (**a**–**f**) DRG sections from *Kcnq4*$^{+/+}$ (**a**,**c**–**f**) and *Kcnq4*$^{-/-}$ (**b**) mice were labeled by immunofluorescence with antibodies specific for KCNQ4 (antibody rbKCNQ4KC in **a**–**d**,**f**; antibody gpKCNQ4A in **e**), NF200 (**a**,**b**), parvalbumin (PV, **c**), c-Ret (**d**) and MafA (**e**). Insets, magnified view of indicated area. (**a**) All neurons expressing KCNQ4 also expressed NF200. Of 860 DRG neurons from eight sections, 10.1 ± 1.1% (s.e.m.) were labeled for KCNQ4. (**b**) KCNQ4 labeling is absent in *Kcnq4*$^{-/-}$ mice. (**c**) KCNQ4-expressing neurons are not labeled for the proprioceptor marker parvalbumin. (**d**) Coexpression of KCNQ4 and c-Ret. Of KCNQ4-positive neurons, 92.7 ± 2.4% also expressed c-Ret (s.e.m., n = 197). (**e**) Coexpression of KCNQ4 and MafA. Of KCNQ4-expressing cells, 89.7 ± 4.3% (s.e.m., n = 116) expressed MafA. (**f**) Retrograde labeling with Alexa Fluor 488–dextran (dextran 488; green, arrow) demonstrates peripheral projection of KCNQ4-expressing DRG neurons (red, arrow) into the skin. Nuclei were labeled with DAPI (blue). Scale bars: 100 μm (**a**–**d**) and 50 μm (**e**,**f**). Boxed areas are magnified in insets.

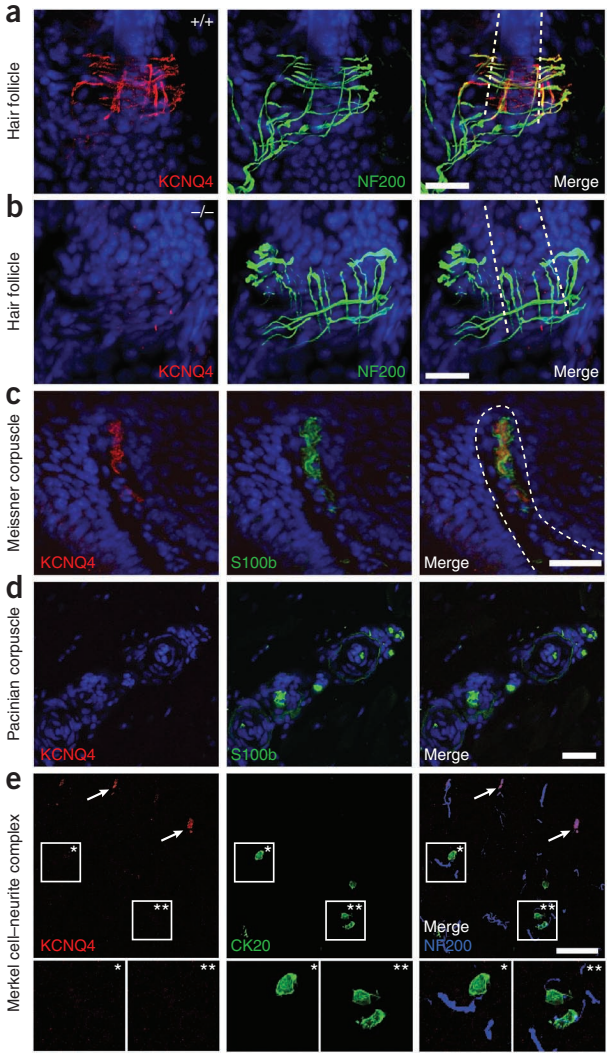

Figure 2 KCNQ4 in mouse skin mechanoreceptors. (**a**) Hairy skin sections stained with antibodies to KCNQ4 (antibody rbKCNQ4KC) and NF200. In WT hair follicles, KCNQ4 labeling is restricted to lanceolate and circular nerve endings. Dashed lines outline hair shaft. (**b**) KCNQ4 labeling is absent in *Kcnq4*$^{-/-}$ mice. Dashed lines outline hair shaft. (**c**) In glabrous skin, KCNQ4 (antibody gpKCNQ4A) localized to S100b-positive nerve endings in Meissner corpuscles (dashed line). (**d**) KCNQ4 is absent from S100b-positive Pacinian corpuscles. Nuclei were labeled with DAPI (blue, **a**–**d**). (**e**) KCNQ4 (antibody gpKCNQ4A) was not detected in complexes of Merkel cell (cytokeratin-20, CK20) and neurite (NF200), but was present in Meissner corpuscles in the same section (arrows). Bottom, magnified views of boxes labeled above with * and **. Scale bars: 20 μm (**a**–**c**), 50 μm (**d**,**e**).

Whereas almost all Meissner corpuscle endings were KCNQ4 positive (33/39), around one-third of hair follicles were found to be KCNQ4-positive (15/43 innervated hair follicles). Notably, in hair follicles innervated by KCNQ4-positive lanceolate endings, only ~50% (87/190) of the S100-positive lanceolate endings were KCNQ4 positive (**Fig. 3a**). Moreover, in hair follicles with KCNQ4-immunoreactive circular fibers (18/30), 71 out of 90 circular, NF200-positive fibers were labeled for KCNQ4. Thus it is likely that distinct mechanoreceptor subtypes, some KCNQ4-positive and others KCNQ4-negative, innervate the same hair follicle.

The co-labeling of KCNQ4 and S100b at lanceolate endings (**Fig. 3a**) raised the question of whether KCNQ4 was expressed in terminal Schwann cells for which S100b is a marker. However, we did not detect KCNQ4 in the cell bodies of Schwann cells, nor were all S100b-positive lanceolate endings of the same Schwann cell positive for KCNQ4 (**Fig. 3a**). High-resolution confocal microscopy revealed that S100b labeling surrounded rather than overlapped with KCNQ4 staining, whereas KCNQ4 staining colocalized with the neuronal marker NF200 (**Fig. 3b**). These data confirmed that KCNQ4 was present in the cell bodies and the peripheral endings of bona fide low-threshold mechanoreceptors.

In hair follicles KCNQ4 protein was restricted to the nerve endings and did not extend proximally to the afferent stem axon (**Supplementary Fig. 3d** and **Supplementary Video 1**). Its localization at, or close to, the impulse generation zone suggested that this K^+ channel might influence stimulus–excitation coupling of rapidly adapting cutaneous mechanoreceptors.

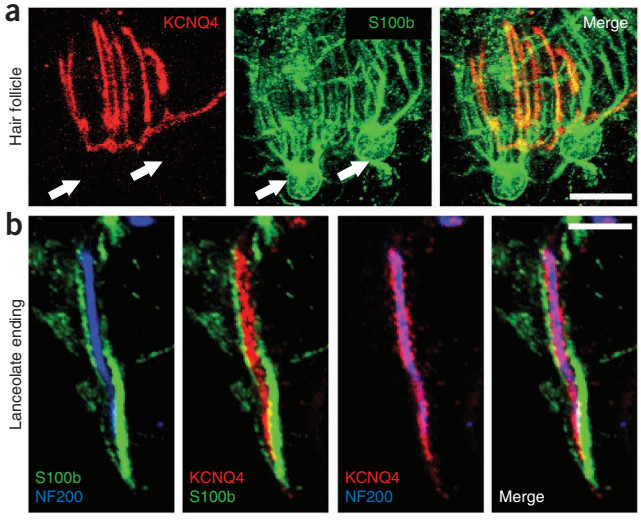

Figure 3 KCNQ4 is absent from terminal Schwann cells in lanceolate endings. (**a**) Stack image of a mouse hair follicle with lanceolate endings stained for KCNQ4 (antibody gpKCNQ4A) and S100b as a marker for Schwann cells. KCNQ4 antibody did not label terminal Schwann cell bodies (arrows). Note that not all S100b-labeled lanceolate endings express KCNQ4. (**b**) Confocal micrograph of a single lanceolate ending labeled for S100b, NF200 and KCNQ4. KCNQ4 is separated from S100b-labeled terminal Schwann cell processes but overlaps with NF200. Scale bars: 10 μm (**a**), 5 μm (**b**).

KCNQ4 dampens rapidly adapting mechanoreceptors

We next used an *in vitro* skin nerve preparation[27,28] to investigate the function of KCNQ4 in mechanoreceptors in mice. Single mechanoreceptors recorded in the saphenous nerve were classified according to their conduction velocity (A-β fibers (RAMs and SAMs), >10 m s^{-1}; thinly myelinated A-δ fibers (D-hair receptor), 1–10 m s^{-1}), von Frey thresholds and their adaptation properties to suprathreshold stimulation[27].

The receptive properties of identified cutaneous mechanoreceptors were tested with repeated ramp-and-hold mechanical stimuli. As described previously, we observed stable non-desensitizing responses to repeated mechanical stimuli in all types of LTM neurons[29,30] (RAMs, D-hairs and SAMs) (**Fig. 4a**–**c**). To test the impact of KCNQ K^+ channels on LTM fiber responses, we exposed their receptive fields to 400 μM of the generic KCNQ channel blocker linopirdine[12,31]. Within minutes of local linopirdine application, both RAMs and D-hairs, but not SAMs, fired faster to the standardized

mechanical stimulus (**Fig. 4a–c**). To test directly whether KCNQ4 is the target for linopirdine in specific mechanoreceptors, we repeated these experiments with mechanoreceptors from *Kcnq4*$^{-/-}$ mice. The linopirdine sensitivity of RAMs, but not of D-hair receptors, was completely lost in mice lacking KCNQ4 (**Fig. 4a,b**). Hence, linopirdine sensitivity of RAMs strictly depends on KCNQ4, whereas different linopirdine-sensitive channels might modulate D-hair responses. These results are consistent with the idea that KCNQ4-negative hair follicle endings belong to D-hair receptors (**Fig. 3a**).

We next used *Kcnq4*$^{dn/+}$ mice, a mouse model[23] for DFNA2 dominant human progressive hearing loss. *Kcnq4*$^{dn/+}$ mice are heterozygous for the G286S mutation, which is equivalent to the G285S mutation identified in humans[12]. KCNQ4^{G285S} subunits exert dominant negative effects on KCNQ4 currents when expressed with wild-type (WT) subunits[12]. Other disease-causing KCNQ4 pore mutants show diminished plasma membrane localization when expressed in heterologous cells[32,33]. We noted that the plasma membrane expression of KCNQ4 was strongly reduced in DRG neurons of *Kcnq4*$^{dn/+}$ mice (**Supplementary Fig. 1b–d**). KCNQ4

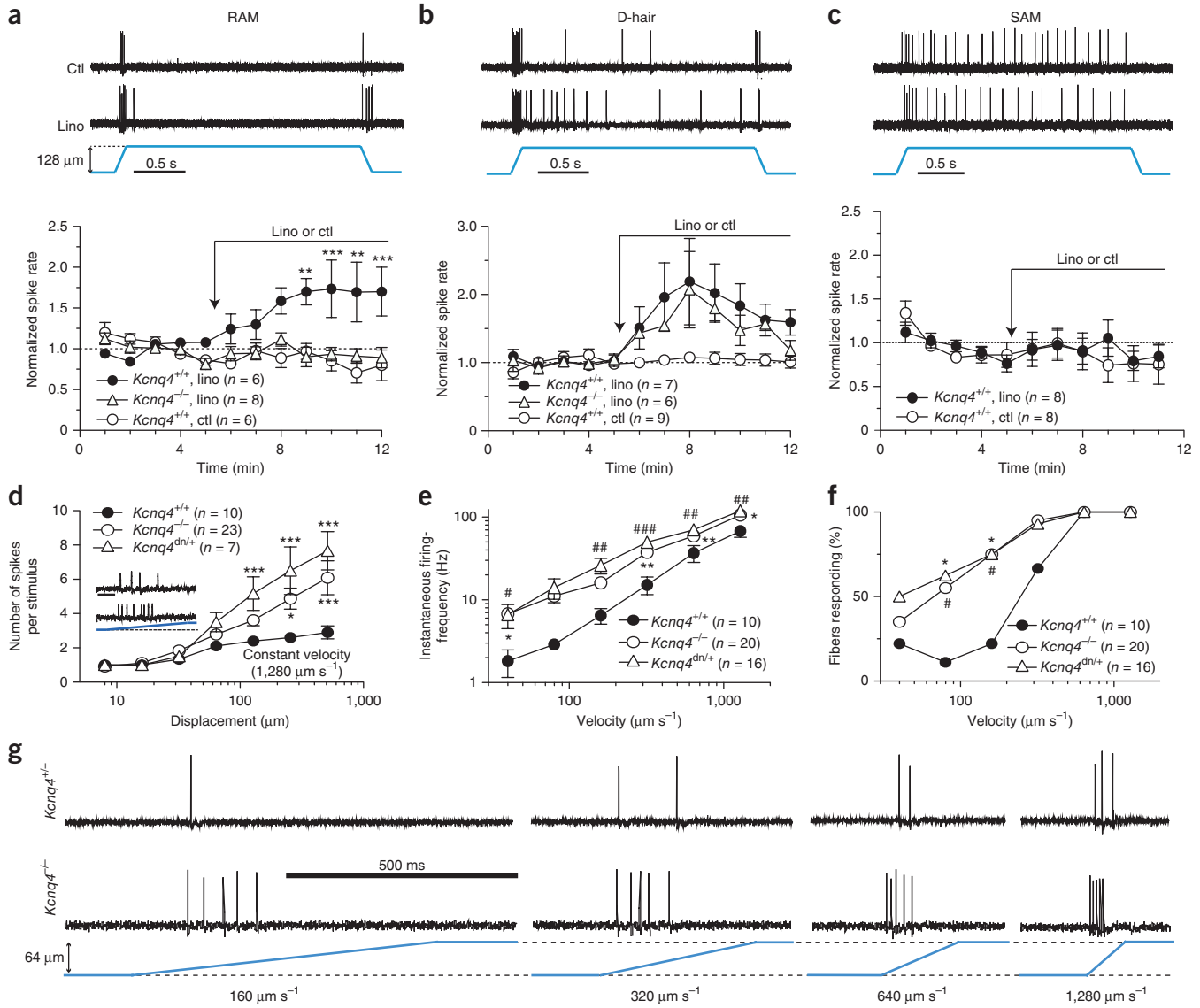

Figure 4 KCNQ4 dampens excitability of RAMs. (**a–c**) Effect of 400 µM linopirdine (lino) on mechanically evoked electrical responses of RAMs (**a**), D-hairs (**b**) and SAMs (**c**) recorded from saphenous nerve of *Kcnq4*$^{+/+}$ and *Kcnq4*$^{-/-}$ mice. Receptive fields of single cutaneous afferents were stimulated with mechanical ramp-and-hold stimuli (2 s duration) at 1-min intervals (typical traces at top). Linopirdine or buffer control (ctl) was added (arrows). Spike rates were normalized to those in the first three responses of each fiber. Note that this normalizes out the higher spike rate of *Kcnq4*$^{-/-}$ mice. Linopirdine sensitivity of RAMs (**a**) but not of D-hairs (**b**) is lost in *Kcnq4*$^{-/-}$ mice ($^{**}P < 0.01$; $^{***}P < 0.001$; Student's *t*-test). (**d**) Spike rates of RAMs during the ramp phase at constant velocities (1,280 µm s^{-1}) as function of displacement amplitudes. Inset: top, *Kcnq4*$^{+/+}$; bottom, *Kcnq4*$^{-/-}$; blue ramp, time course of indentation; scale bar, 20 ms. *Kcnq4*$^{-/-}$ and *Kcnq4*$^{dn/+}$ RAMs fired more spikes than RAMs from WT littermate controls ($^{*}P < 0.05$; $^{***}P < 0.001$; Student's *t*-test). (**e**) Mean instantaneous firing frequencies as function of stimulus velocity at constant stimulus amplitude (64 µm). *Kcnq4*$^{-/-}$ and *Kcnq4*$^{dn/+}$ mice had higher firing frequencies than WT littermate controls (**Kcnq4*$^{-/-}$, $^{\#}$*Kcnq4*$^{dn/+}$; $^{*,\#}P < 0.05$, $^{**,\#\#}P < 0.01$, $^{\#\#\#}P < 0.001$; Student's *t*-test). (**f**) Proportions of fibers from WT, *Kcnq4*$^{-/-}$ and *Kcnq4*$^{dn/+}$ mice responding to stimuli of a given velocity. Proportions were compared using Fisher's exact test ($^{*}P < 0.05$, *Kcnq4*$^{dn/+}$; $^{\#}P < 0.05$, *Kcnq4*$^{-/-}$; compared to *Kcnq4*$^{+/+}$). (**g**) Examples traces of RAM spike bursts evoked by different stimulation velocities in WT and *Kcnq4*$^{-/-}$ mice. Error bars are s.e.m.

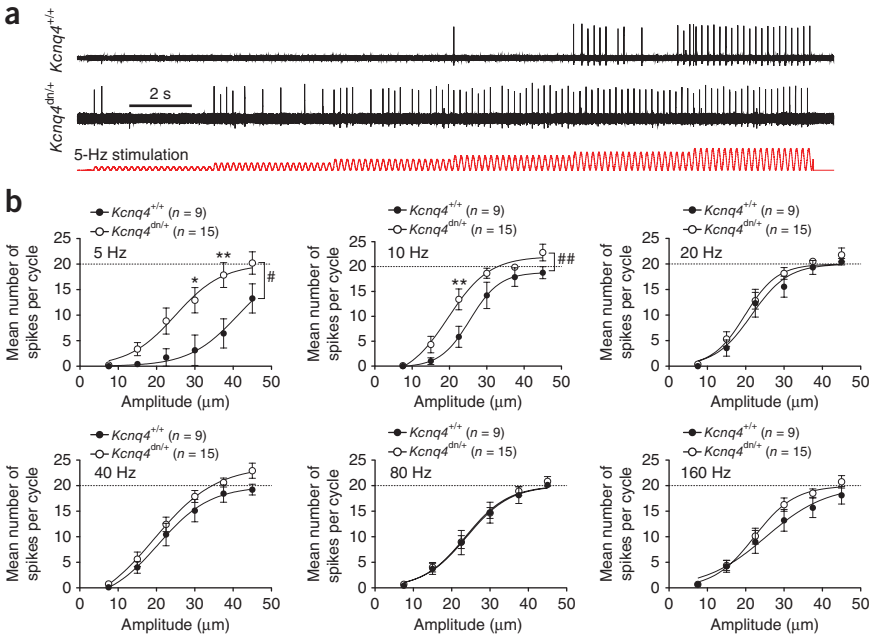

Figure 5 Altered frequency tuning in *Kcnq4*$^{dn/+}$ mice. (**a**,**b**) RAMs were stimulated with sinusoidal vibration stimuli over a range of frequencies (5–160 Hz) with vibration amplitudes being increased from 7.5 μm to 45 μm in steps of 7.5 μm after periods of 20 cycles. (**a**) Example responses of *Kcnq4*$^{+/+}$ and *Kcnq4*$^{dn/+}$ RAMs to a 5-Hz stimulation are shown in black. Red trace shows the mechanical stimulation protocol. (**b**) Mean number of spikes per cycle plotted as function of vibration amplitude for 5, 10, 20, 40, 80 and 160 Hz. At 5 and 10 Hz, *Kcnq4*$^{dn/+}$ mice were significantly more sensitive than littermate controls ($^{\#}P < 0.05$, $^{\#\#}P < 0.01$, two-way repeated-measures ANOVA; $^{*}P < 0.05$, $^{**}P < 0.01$, Bonferroni post-test). Dashed lines indicate one spike per cycle. Error bars are s.e.m.

protein was also strongly reduced in cutaneous nerve endings of *Kcnq4*$^{dn/+}$ mice and nearly absent from *Kcnq4*$^{dn/dn}$ nerve endings (**Supplementary Figs. 1e**,**f** and **3e**–**h**). These results suggest that disease-causing KCNQ4 pore mutations exert dominant negative effects by affecting the trafficking of homomeric and heteromeric channels containing mutant subunits.

Consistent with the effect of linopirdine (**Fig. 4a**–**c**), RAMs from *Kcnq4*$^{dn/+}$ and *Kcnq4*$^{-/-}$ mice fired more spikes in response to step displacements (applied at a constant ramp velocity) than RAMs recorded from *Kcnq4*$^{+/+}$ littermates (**Fig. 4d**). In contrast, the responses of SAMs and D-hair receptors were the same in *Kcnq4*$^{dn/+}$ and *Kcnq4*$^{-/-}$ mutant mice as in controls (**Supplementary Fig. 4a**,**b**). RAMs lacking KCNQ4 not only fired more spikes but also showed shorter interspike intervals (**Fig. 4d**, inset). Von Frey thresholds, axonal conduction velocities and the proportions of RAMs and SAMs among A-β fibers were not affected by the lack of KCNQ4 (**Supplementary Fig. 4c**–**e**).

As the firing frequency of RAMs encodes the velocity of a mechanical stimulus, we stimulated RAMs with ramp-and-hold displacements of variable ramp speeds but constant hold amplitudes (**Fig. 4e**–**g**). As observed in other mouse strains[28] and in primates[6], RAM firing frequencies faithfully encoded velocity. However, *Kcnq4*$^{+/+}$ RAMs rarely detected slow ramp indentations (<400 μm s^{-1}), whereas both *Kcnq4*$^{-/-}$ and *Kcnq4*$^{dn/+}$ RAMs reliably responded to such stimuli (**Fig. 4f**) and typically showed between two- and fivefold higher instantaneous firing frequencies (that is, shorter interspike intervals) than controls at all tested velocities (**Fig. 4e**,**g**).

To investigate the impact of KCNQ4 on frequency preference, we recorded the response of RAMs from *Kcnq4*$^{+/+}$ and *Kcnq4*$^{dn/+}$ mice to sinusoidal stimuli of increasing amplitudes over a wide range of frequencies (5–180 Hz) (**Fig. 5**). *Kcnq4*$^{dn/+}$ RAMs responded normally to high-frequency stimulation, but they were more sensitive than controls at 10 Hz and even more so at 5 Hz (**Fig. 5**). For instance, vibration amplitudes of ~20 μm elicited the same firing rate in *Kcnq4*$^{dn/+}$ RAMs as ~40 μm amplitudes in WT RAMs. These data support the hypothesis that KCNQ4 channels dampen the response of rapidly adapting hair follicle and Meissner corpuscle afferents and tune these mechanoreceptors to higher frequencies for normal touch sensation in mice.

It could be argued that lack of KCNQ4 function may lead to mechanoreceptor degeneration, akin to the loss of cochlear outer hair cells observed in *Kcnq4* mutant mice[23]. We used immunohistochemistry to compare the number and morphology of mechanoreceptors from *Kcnq4*$^{+/+}$ mice with those of *Kcnq4*$^{dn/+}$ mice. The latter, though

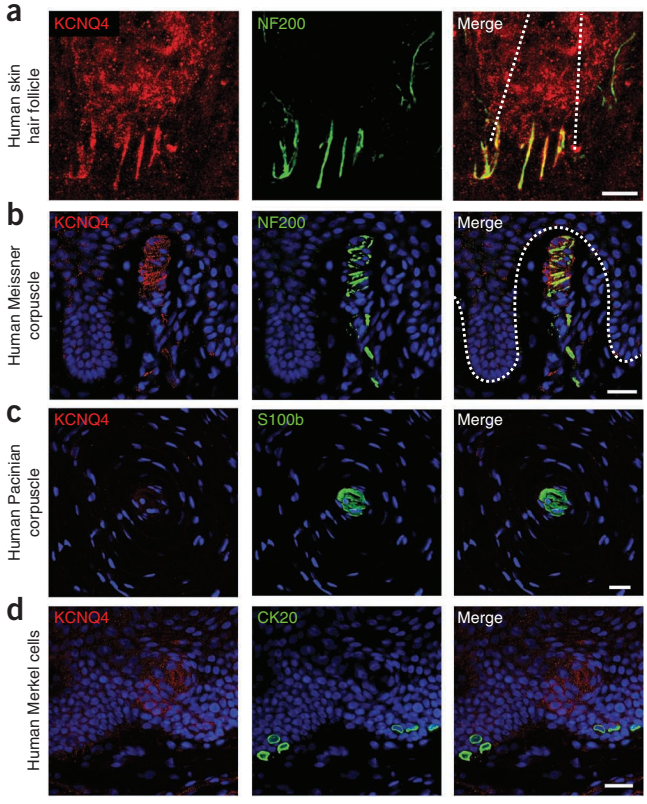

Figure 6 KCNQ4 in human skin mechanoreceptors. (**a**–**d**) Human skin sections stained with antibodies to KCNQ4 (antibody rbKCNQ4KC), NF200, S100b and CK20. (**a**) KCNQ4 labeling of lanceolate endings in human hair follicles. Dotted lines outline hair shaft. (**b**) KCNQ4 localized to nerve endings in Meissner corpuscles (dotted line). (**c**) KCNQ4 was not detected in S100b-positive Pacinian corpuscles. (**d**) KCNQ4 was absent from CK20-positive Merkel cell complexes. Nuclei were labeled with DAPI (blue) in **b**–**d**. Scale bars, 20 μm.

lacking KCNQ4 currents, can be identified by KCNQ4 labeling (**Supplementary Fig. 1c**,**e**). Neither the morphology of KCNQ4-positive hair follicle afferents and Meissner corpuscles (**Supplementary Fig. 3e**–**h**) nor the number of KCNQ4-positive DRG neurons (**Supplementary Fig. 5a**,**b**) was altered. There was also no loss of large myelinated fibers, as determined from counts made from semi-thin sections of the saphenous nerves of *Kcnq4*$^{+/+}$ and *Kcnq4*$^{dn/+}$ mice (**Supplementary Fig. 5c**,**d**). Examination of electron micrographs of large myelinated fibers also revealed no anatomical abnormalities in nerves taken from *Kcnq4*$^{dn/+}$ mice (**Supplementary Fig. 5c**).

KCNQ4 loss enhances detection of low-frequency vibration

To explore the behavioral consequences of altered mechanosensitivity, we used a tactile acuity test (**Supplementary Fig. 6a**). This two-choice preference test ('grid test')[34] tests the ability of mice to detect a grating cue placed on the floor of an arena. On the mixed CBA/J and C57Bl/6J genetic background used for these experiments, *Kcnq4*$^{dn/+}$ mutant mice spent significantly ($P < 0.05$) more time on grids than on control areas, whereas there was no significant difference for *Kcnq4*$^{+/+}$ littermate controls (**Supplementary Fig. 6b**). But although these results suggested that *Kcnq4*$^{dn/+}$ mice recognized grids better than WT, a direct comparison between these genotypes did not yield a significant difference. We compared *Kcnq4*$^{-/-}$ and *Kcnq4*$^{+/+}$ mice in an inbred CH3 background. Mice of either genotype similarly recognized the grid (**Supplementary Fig. 6c**). However, this behavioral assay does not specifically test for the ability to discriminate vibrotactile stimuli and is influenced by other mechanoreceptors not expressing KCNQ4.

Vibrotactile discrimination can be conveniently studied and quantified in humans. Co-labeling human skin biopsy sections with antibodies to KCNQ4 and NF200 showed KCNQ4 protein in human lanceolate endings and Meissner corpuscles (**Fig. 6a**,**b**), similar to that observed in mice (**Fig. 2a**,**c** and **Supplementary Fig. 3**). Likewise, we detected no KCNQ4 protein in Pacinian corpuscles and Merkel cell complexes in human skin (**Fig. 6c**,**d**).

We then examined touch sensitivity in people from two DFNA2 pedigrees carrying two different *KCNQ4* mutations (G296S and W276S; refs. 32,35) (**Fig. 7** and **Supplementary Fig. 7a**,**b**). Both mutations studied exert dominant negative effects like that of the G285S mutation[12] on which *Kcnq4*$^{dn/+}$ mice were modeled[23]. To assess the function of vibration-sensitive RAM subtypes (that is, Meissner corpuscles and Pacinian corpuscles), we measured vibrotactile thresholds over a broad frequency range (5–160 Hz) using an ascending method of limits approach (**Fig. 7a**, top). Meissner corpuscles and hair follicle afferents, which both express KCNQ4 (**Figs. 2a**,**c** and **6a**,**b**), are the primary detectors of low-frequency vibrotactile stimuli, whereas high frequencies are primarily detected by Pacinian corpuscles (**Fig. 7a**, top)[1,6,36]. In a large cohort of adults with DFNA2 (37–55 years old), vibration detection thresholds were significantly lower at 5 and 10 Hz but not at higher frequencies than those in healthy, age-matched controls (**Fig. 7a**, bottom). Differences in vibrotactile acuity were even more pronounced when we directly compared data obtained from affected individuals with data from their healthy siblings (~50% threshold reduction at 5 and 10 Hz; **Fig. 7c**–**e**). We also examined vibration detection thresholds at 125 Hz with a forced-choice test using a commercial system. In agreement with the ascending method

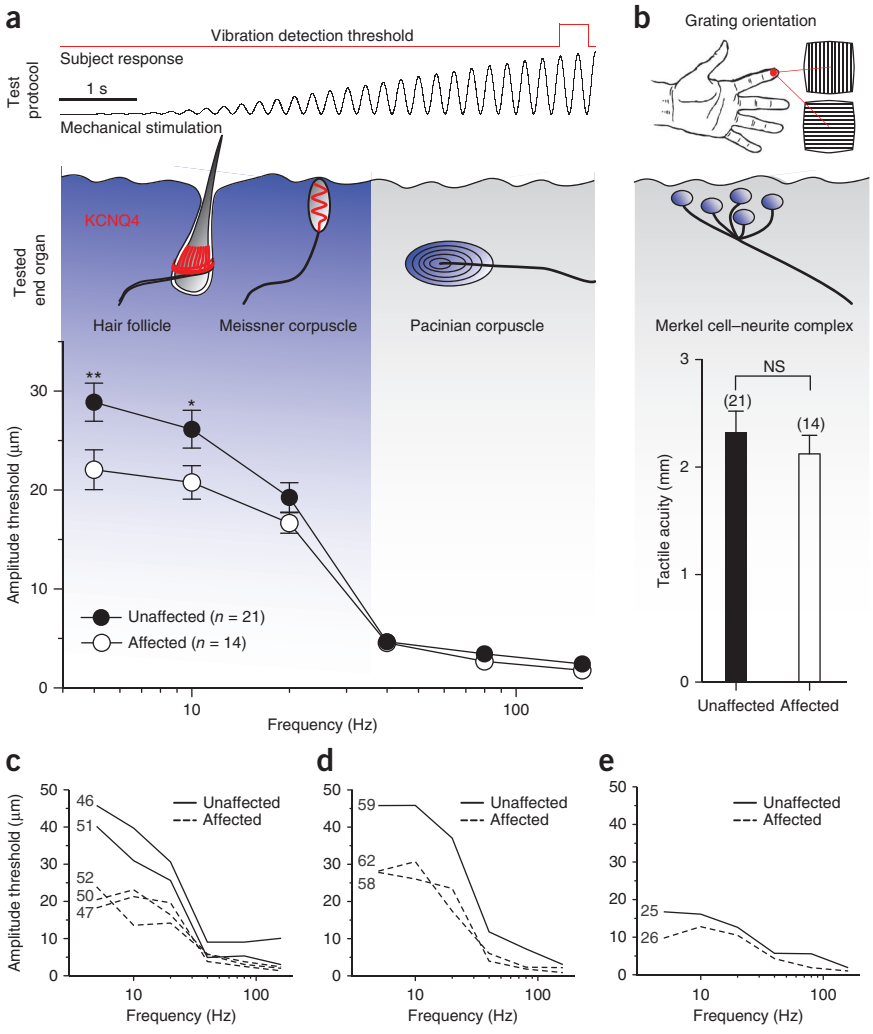

Figure 7 Enhanced detection of low-frequency vibrations in subjects with DFNA2 carrying *KCNQ4* mutations. (**a**) Top (test procedure): subjects signaled the detection of vibratory stimuli (black trace) by pressing a button (red trace). Middle (tested end organ): the frequency ranges for optimal activation of Meissner and Pacinian corpuscles. Bottom: mean vibration detection thresholds in subjects with DFNA2 (affected) and controls (unaffected) at 5, 10, 20, 40, 80 and 160 Hz. (*$P < 0.05$; **$P < 0.01$; two-way repeated measures ANOVA, Bonferroni post-test). (**b**) Top (test procedure): subjects had to detect whether a grating was pressed in longitudinal or transverse orientation against their finger. Middle (tested end organ): Merkel cell–neurite complexes are tested. Bottom: comparison of the limits of spatial resolutions in the index fingers of subjects with DFNA2 and age-matched healthy controls. No significant difference was observed (NS; $P = 0.47$, Student's *t*-test; *n* values in parentheses). (**c**–**e**) Comparison of individual vibrotactile tuning curves of affected (dashed lines) and unaffected (solid lines) subjects from three different sibships. Subject identifiers are the same as used when previously published[35] and are indicated in the pedigree in **Supplementary Figure 7**. Error bars are s.e.m.

of limits approach, we observed no significant difference in detection thresholds at 125 Hz between subjects with DFNA2 and controls (**Supplementary Fig. 7c**).

To assess the function of SAMs (that is, Merkel cell–neurite complexes), which in mice (**Fig. 2e**) and humans (**Fig. 6d**) do not express KCNQ4, we determined the limits of spatial resolution in the fingertip using a two-interval forced-choice tactile grating orientation test (**Fig. 7b**, top)[37,38]. We detected no difference between subjects with DFNA2 and controls (**Fig. 7b**, bottom).

DISCUSSION

Here we show that KCNQ4 is a functionally relevant marker of a specific type of RAM in mice and in humans. KCNQ4 protein is targeted to the peripheral endings of defined mechanoreceptors in the skin, where it is localized to a region juxtaposed to the transduction zone. We show directly that the KCNQ4 channel is required for tuning the coding of vibrotactile stimuli so that low-frequency sinusoids (<10 Hz) are more poorly detected than higher frequencies. Accordingly, loss of KCNQ4 function leads to a selective enhancement of mechanoreceptor sensitivity to low-frequency vibration. Notably, people with late-onset hearing loss due to dominant mutations of the *KCNQ4* gene show enhanced performance in detecting small-amplitude, low-frequency vibration. Thus our data provide a direct link between a hearing gene and human touch sensitivity.

The Meissner touch corpuscle (described by Georg Meissner in 1853) has long been known to be the end organ of RAMs in human glabrous skin. Human microneurography studies classically differentiate two main types of RAMs: RA-type I, identical with Meissner type mechanoreceptors in glabrous skin; and RA-type II, which are identical to Pacinian corpuscle receptors (described by Filippo Pacini in 1840)[36,39]. These two types of receptor differ profoundly in their physiological properties, one key difference being that Pacinian receptors are tuned to detect high-frequency vibration (>100 Hz) with high sensitivity, whereas type I RAMs have an optimal range of sensitivity at lower frequencies (middle range 10–40 Hz)[1,6]. In both mice and humans, the KCNQ4 protein is present in Meissner corpuscles (RA-type I) but not in Pacinian corpuscles (RA-type II).

In hairy skin, RAMs activated by hair movement are likely functionally equivalent to type I receptors[40,41]. We show that the KCNQ4 protein is localized to lanceolate endings that form a basket-like structure at the base of human and mouse hair follicles. These endings detect hair movement, and the transduction channels are presumably localized at such endings. Our finding that hair follicles in the mouse are innervated by both KCNQ4-positive and KCNQ4-negative lanceolate endings constitutes direct evidence that individual hairs are innervated by functionally distinct RAMs. Indeed, we found the linopirdine sensitivity of D-hair receptors to be independent of KCNQ4, suggesting that D-hair receptors are KCNQ4-negative and thus that individual mouse hairs may be innervated by both RAMs and D-hair receptor lanceolate endings.

We show that KCNQ4 channels are located at sites that overlap with or are directly adjacent to probable sites of mechanoelectric transduction[29]. Thus KCNQ4 channels are ideally placed to regulate the transformation of receptor potentials to spike trains at their origin. The manner in which the receptor potential is converted into a spike train is not well understood[42–44]. We show here that KCNQ4 channels specifically control the excitability of a functionally distinct subset of RAMs. KCNQ channels lack mechanosensitivity[45], and we have confirmed this experimentally (**Supplementary Fig. 8**). KCNQ channels are non-inactivating and are partially open at negative potentials, thereby contributing to the clamping of the resting membrane potential[46]. Indeed, cochlear outer hair cells of *Kcnq4* mutant mice are depolarized[23]. Thus a likely explanation for the increased sensitivity of RAMs lacking KCNQ4 is a depolarized resting membrane potential closer to the action potential firing threshold. The KCNQ4-dependent changes in sensitivity are much more pronounced with slow stimuli; consequently, the tuning of RAMs to higher frequency vibration (>10 Hz) is markedly attenuated in $Kcnq4^{dn/+}$ and $Kcnq4^{-/-}$ mutant mice. This effect may be explained by KCNQ4-dependent conductive shunting, which, compared to capacitative shunting, is much more effective at low frequencies.

In contrast to the limited data available from rodents, there are many quantitative studies on vibrotactile behavior in humans, and so we sought to assess the effect of *KCNQ4* loss of function alleles in humans with DFNA2. Notably, the observed frequency tuning of RAMs in mice matches the psychometric function of humans and nonhuman primates to vibrotactile stimuli[6,39,47,48]. Humans are much better at detecting small-amplitude vibrotactile stimuli applied to the skin at frequencies >20 Hz than <20 Hz. Thus larger stimulus amplitudes are required for low-frequency vibration before the subject is able to perceive the stimulus[36]. High-frequency vibrations are detected primarily by Pacinian corpuscle afferents (type II RAMs), whereas low-frequency vibrations are detected by Meissner corpuscles[1,6], which we found to express KCNQ4 in mice and humans. Here we have shown, with two distinct kindreds with DFNA2 (refs. 32,35), that the presence of mutations that reduce KCNQ4 currents shifts the psychometric tuning curve so that individuals with DFNA2 are better than age-matched controls at detecting low frequency skin vibration . Of note, the behavioral performance of the subjects with DFNA2 was normal for very high frequency stimuli, detected by Pacinian receptors, which lack KCNQ4 immunoreactivity.

It is not clear whether people with DFNA2 reap a behavioral benefit or disadvantage from their enhanced sensitivity to slow-moving stimuli. One theory postulates that type I RAMs primarily sense slip forces to enable precise grip control[49]. However, it is also clear that different mechanoreceptors act in an ensemble during different phases of complex tasks[49]. It has been proposed that it is spike timing rather than spike frequency that provides relevant information about tactile stimulus direction and velocity[50]. The absence of KCNQ4 in skin mechanoreceptors would lead to a substantial change in the temporal order of spikes from type I RAM afferents at lower velocities of skin stimulation. Researchers working on human touch have used methods such as microneurography to provide models of how behaviorally relevant tactile information is coded. Nevertheless, until now there were no experimental tools available to directly manipulate the mechanoreceptor coding of sensory stimuli and test the consequences for behavior. Our work demonstrates that a direct manipulation of mechanoreceptor coding is possible.

In summary, we have identified KCNQ4 as a functionally relevant marker of RAMs in mice and in man. The critical role of this K^+ channel in hearing has been known for years[12], and we now show that it is also important in modulating touch sensitivity. Whereas the loss of KCNQ4 causes deafness[12] mainly by precipitating the degeneration of sensory hair cells[23], it instead increases touch sensitivity at low frequencies. We have identified KCNQ4 as a crucial element in tuning mechanoreceptors to detect specific tactile stimuli.

METHODS

Methods and any associated references are available in the online version of the paper at http://www.nature.com/natureneuroscience/.

Note: Supplementary information is available on the Nature Neuroscience website.

ACKNOWLEDGMENTS

We thank P. Seidler and H. Thraenhardt for technical assistance, the DFNA2 families for their collaboration, C. Birchmeier (MDC Berlin) for the MafA antibody, M. Maurer (Charité Berlin) for human skin biopsies and B. Purfuerst for electron microscopy. Supported by an SAW (Senatsausschuss Wettbewerb) grant of the Leibniz Gemeinschaft to T.J.J. and G.R.L., the Prix Louis-Jeantet de Médecine and the Ernst-Jung Preis für Medizin to T.J.J. and grants from the Deutsche Forschungsgemeinschaft (DFG) (SFB665) to G.R.L.; additional funding (T.J.J. and G.R.L.) was provided by the DFG (Exc 257 NeuroCure).

AUTHOR CONTRIBUTIONS

M.H. performed and evaluated morphological and mouse behavioral studies, examined subjects and wrote the paper; S.G.L. performed and evaluated electrophysiological experiments, designed and built psychometric tests, examined subjects and wrote the paper; V.V. did initial antibody characterization and DRG staining; C.W. established mouse behavioral studies and analyzed electron micrographs; C.W.C., E.M.D.L., M.A.M.-P. and G.A. organized human studies; T.J.J. initiated the project, designed and evaluated experiments, organized human studies and wrote the paper; G.R.L. designed and evaluated experiments and wrote the paper.

COMPETING FINANCIAL INTERESTS

The authors declare no competing financial interests.

Published online at http://www.nature.com/natureneuroscience/.
Reprints and permissions information is available online at http://www.nature.com/reprints/index.html.

1. Johnson, K.O. The roles and functions of cutaneous mechanoreceptors. *Curr. Opin. Neurobiol.* **11**, 455–461 (2001).
2. Lewin, G.R. & Moshourab, R. Mechanosensation and pain. *J. Neurobiol.* **61**, 30–44 (2004).
3. Loewenstein, W.R. & Rathkamp, R. The sites for mechano-electric conversion in a Pacinian corpuscle. *J. Gen. Physiol.* **41**, 1245–1265 (1958).
4. Maricich, S.M. *et al.* Merkel cells are essential for light-touch responses. *Science* **324**, 1580–1582 (2009).
5. Blake, D.T., Hsiao, S.S. & Johnson, K.O. Neural coding mechanisms in tactile pattern recognition: the relative contributions of slowly and rapidly adapting mechanoreceptors to perceived roughness. *J. Neurosci.* **17**, 7480–7489 (1997).
6. Talbot, W.H., Darian-Smith, I., Kornhuber, H.H. & Mountcastle, V.B. The sense of flutter-vibration: comparison of the human capacity with response patterns of mechanoreceptive afferents from the monkey hand. *J. Neurophysiol.* **31**, 301–334 (1968).
7. Bensmaïa, S.J. & Hollins, M. The vibrations of texture. *Somatosens. Mot. Res.* **20**, 33–43 (2003).
8. Brown, D.A. & Passmore, G.M. Neural KCNQ (Kv7) channels. *Br. J. Pharmacol.* **156**, 1185–1195 (2009).
9. Biervert, C. *et al.* A potassium channel mutation in neonatal human epilepsy. *Science* **279**, 403–406 (1998).
10. Kharkovets, T. *et al.* KCNQ4, a K^+ channel mutated in a form of dominant deafness, is expressed in the inner ear and the central auditory pathway. *Proc. Natl. Acad. Sci. USA* **97**, 4333–4338 (2000).
11. Tzingounis, A.V. *et al.* The KCNQ5 potassium channel mediates a component of the afterhyperpolarization current in mouse hippocampus. *Proc. Natl. Acad. Sci. USA* **107**, 10232–10237 (2010).
12. Kubisch, C. *et al.* KCNQ4, a novel potassium channel expressed in sensory outer hair cells, is mutated in dominant deafness. *Cell* **96**, 437–446 (1999).
13. Schroeder, B.C., Hechenberger, M., Weinreich, F., Kubisch, C. & Jentsch, T.J. KCNQ5, a novel potassium channel broadly expressed in brain, mediates M-type currents. *J. Biol. Chem.* **275**, 24089–24095 (2000).
14. Yeung, S.Y.M. *et al.* Molecular expression and pharmacological identification of a role for K(v)7 channels in murine vascular reactivity. *Br. J. Pharmacol.* **151**, 758–770 (2007).
15. Wang, H.S. *et al.* KCNQ2 and KCNQ3 potassium channel subunits: molecular correlates of the M-channel. *Science* **282**, 1890–1893 (1998).
16. Selyanko, A.A. *et al.* Inhibition of KCNQ1–4 potassium channels expressed in mammalian cells via M1 muscarinic acetylcholine receptors. *J. Physiol. (Lond.)* **522**, 349–355 (2000).
17. Lechner, S.G., Mayer, M. & Boehm, S. Activation of M1 muscarinic receptors triggers transmitter release from rat sympathetic neurons through an inhibition of M-type K^+ channels. *J. Physiol. (Lond.)* **553**, 789–802 (2003).
18. Charlier, C. *et al.* A pore mutation in a novel KQT-like potassium channel gene in an idiopathic epilepsy family. *Nat. Genet.* **18**, 53–55 (1998).
19. Peters, H.C., Hu, H., Pongs, O., Storm, J.F. & Isbrandt, D. Conditional transgenic suppression of M channels in mouse brain reveals functions in neuronal excitability, resonance and behavior. *Nat. Neurosci.* **8**, 51–60 (2005).
20. Watanabe, H. *et al.* Disruption of the epilepsy KCNQ2 gene results in neural hyperexcitability. *J. Neurochem.* **75**, 28–33 (2000).
21. Passmore, G.M. *et al.* KCNQ/M currents in sensory neurons: significance for pain therapy. *J. Neurosci.* **23**, 7227–7236 (2003).
22. Linley, J.E. *et al.* Inhibition of M current in sensory neurons by exogenous proteases: a signaling pathway mediating inflammatory nociception. *J. Neurosci.* **28**, 11240–11249 (2008).
23. Kharkovets, T. *et al.* Mice with altered KCNQ4 K^+ channels implicate sensory outer hair cells in human progressive deafness. *EMBO J.* **25**, 642–652 (2006).
24. Bourane, S. *et al.* Low-threshold mechanoreceptor subtypes selectively express MafA and are specified by Ret signaling. *Neuron* **64**, 857–870 (2009).
25. Luo, W., Enomoto, H., Rice, F.L., Milbrandt, J. & Ginty, D.D. Molecular identification of rapidly adapting mechanoreceptors and their developmental dependence on ret signaling. *Neuron* **64**, 841–856 (2009).
26. Bolanowski, S.J. & Zwislocki, J.J. Intensity and frequency characteristics of pacinian corpuscles. I. Action potentials. *J. Neurophysiol.* **51**, 793–811 (1984).
27. Koltzenburg, M., Stucky, C.L. & Lewin, G.R. Receptive properties of mouse sensory neurons innervating hairy skin. *J. Neurophysiol.* **78**, 1841–1850 (1997).
28. Milenkovic, N., Wetzel, C., Moshourab, R. & Lewin, G.R. Speed and temperature dependences of mechanotransduction in afferent fibers recorded from the mouse saphenous nerve. *J. Neurophysiol.* **100**, 2771–2783 (2008).
29. Hu, J., Chiang, L.-Y., Koch, M. & Lewin, G.R. Evidence for a protein tether involved in somatic touch. *EMBO J.* **29**, 855–867 (2010).
30. Lechner, S.G. & Lewin, G.R. Peripheral sensitisation of nociceptors via G-protein-dependent potentiation of mechanotransduction currents. *J. Physiol. (Lond.)* **587**, 3493–3503 (2009).
31. Søgaard, R., Ljungstrøm, T., Pedersen, K.A., Olesen, S.P. & Jensen, B.S. KCNQ4 channels expressed in mammalian cells: functional characteristics and pharmacology. *Am. J. Physiol. Cell Physiol.* **280**, C859–C866 (2001).
32. Mencía, A. *et al.* A novel KCNQ4 pore-region mutation (p.G296S) causes deafness by impairing cell-surface channel expression. *Hum. Genet.* **123**, 41–53 (2008).
33. Kim, H.J., Lv, P., Sihn, C.-R. & Yamoah, E.N. Cellular and molecular mechanisms of autosomal dominant form of progressive hearing loss, DFNA2. *J. Biol. Chem.* **286**, 1517–1527 (2011).
34. Wetzel, C. *et al.* A stomatin-domain protein essential for touch sensation in the mouse. *Nature* **445**, 206–209 (2007).
35. De Leenheer, E.M.R. *et al.* Longitudinal and cross-sectional phenotype analysis in a new, large Dutch DFNA2/KCNQ4 family. *Ann. Otol. Rhinol. Laryngol.* **111**, 267–274 (2002).
36. Johansson, R.S. & Vallbo, A.B. Detection of tactile stimuli. Thresholds of afferent units related to psychophysical thresholds in the human hand. *J. Physiol. (Lond.)* **297**, 405–422 (1979).
37. Van Boven, R.W. & Johnson, K.O. The limit of tactile spatial resolution in humans: grating orientation discrimination at the lip, tongue, and finger. *Neurology* **44**, 2361–2366 (1994).
38. Bensmaia, S.J., Denchev, P.V., Dammann, J.F., Craig, J.C. & Hsiao, S.S. The representation of stimulus orientation in the early stages of somatosensory processing. *J. Neurosci.* **28**, 776–786 (2008).
39. Knibestöl, M. Stimulus–response functions of rapidly adapting mechanoreceptors in the human glabrous skin area. *J. Physiol. (Lond.)* **232**, 427–452 (1973).
40. Vallbo, A.B., Olausson, H., Wessberg, J. & Kakuda, N. Receptive field characteristics of tactile units with myelinated afferents in hairy skin of human subjects. *J. Physiol. (Lond.)* **483**, 783–795 (1995).
41. Trulsson, M. & Essick, G.K. Sensations evoked by microstimulation of single mechanoreceptive afferents innervating the human face and mouth. *J. Neurophysiol.* **103**, 1741–1747 (2010).
42. Hu, J. & Lewin, G.R. Mechanosensitive currents in the neurites of cultured mouse sensory neurones. *J. Physiol. (Lond.)* **577**, 815–828 (2006).
43. Tsunozaki, M. & Bautista, D.M. Mammalian somatosensory mechanotransduction. *Curr. Opin. Neurobiol.* **19**, 362–369 (2009).
44. French, A.S. & Torkkeli, P.H. Mechanotransduction in spider slit sensilla. *Can. J. Physiol. Pharmacol.* **82**, 541–548 (2004).
45. Hammami, S. *et al.* Cell volume and membrane stretch independently control K^+ channel activity. *J. Physiol. (Lond.)* **587**, 2225–2231 (2009).
46. Jentsch, T.J. Neuronal KCNQ potassium channels: physiology and role in disease. *Nat. Rev. Neurosci.* **1**, 21–30 (2000).
47. Darian-Smith, I., Davidson, I. & Johnson, K.O. Peripheral neural representation of spatial dimensions of a textured surface moving across the monkey's finger pad. *J. Physiol. (Lond.)* **309**, 135–146 (1980).
48. Knibestöl, M. Stimulus-response functions of slowly adapting mechanoreceptors in the human glabrous skin area. *J. Physiol. (Lond.)* **245**, 63–80 (1975).
49. Johansson, R.S. & Flanagan, J.R. Coding and use of tactile signals from the fingertips in object manipulation tasks. *Nat. Rev. Neurosci.* **10**, 345–359 (2009).
50. Johansson, R.S. & Birznieks, I. First spikes in ensembles of human tactile afferents code complex spatial fingertip events. *Nat. Neurosci.* **7**, 170–177 (2004).

ONLINE METHODS

Mice. All mice were housed in the animal facility of the MDC Berlin according to institutional guidelines. All animal experiments were done according to the German Animal Protection Law. *Kcnq4*$^{-/-}$ and *Kcnq4*$^{dn/+}$mice used in our study have been described in detail[23]. *Kcnq4*$^{-/-}$ mice were backcrossed to a C3H background (>10 generations). *Kcnq4*$^{dn/+}$ mice were analyzed on a mixed background (CBA/J and C57Bl/6J). For all experiments shown in **Figure 4** and **Supplementary Figures 4** and **5**, *Kcnq4*$^{+/+}$ mice on a pure C3H background were used as controls. For experiments shown in **Figure 5** and **Supplementary Figure 6** *Kcnq4*$^{+/+}$ littermates (mixed background: CBA/J and C57Bl/6J) served as controls.

Humans. Two DFNA2 pedigrees, which carry two different *KCNQ4* mutations (G296S and W276S)[32,35], were examined. Owing to large age-dependent inter-individual variations, children were excluded from the analysis and only adults aged 37–55 year were considered. When both were available, subjects with DFNA2 and their healthy siblings were tested. Unrelated healthy age-matched subjects served as additional controls. Informed consent was obtained from all subjects before examination. All experiments were undertaken with written consent of each person.

Immunohistochemistry. Mice were anesthetized with ketamine and rompun and perfused through the heart with 4% (wt/vol) paraformaldehyde (PFA) in PBS. For guinea pig anti-KCNQ4 labeling, the PFA concentration was reduced to 1%. For MafA labeling, mice 6 d (**Fig. 2**) and 20 weeks old (**Supplementary Fig. 5**) were used. Mouse tissues were dissected and postfixed with 4% or 1% PFA, as appropriate, for 30 min at 4 °C. DRGs and spinal cords were incubated overnight in 30% (wt/vol) sucrose at 4 °C and embedded in Tissue Tek O.C.T. (Sakura). Cryosections were cut at 8 µm (for spinal cords, Pacinian corpuscles and DRGs) and 30–40 µm (for skin). For Pacinian corpuscle staining, the distal halves of mouse legs containing interosseous membranes were dissected, postfixed in 1% PFA for 30 min, washed with PBS and decalcified with EDTA for 2–3 d. Human skin biopsies were immediately placed in 4% PFA after dissection and fixed for 48 h at 4 °C followed by incubation in 30% sucrose for 48 h at 4 °C and OCT embedding. Sections 30 µm were cut. Tissues were blocked in 3% (vol/vol) normal goat serum, 2% (wt/vol) BSA and 0.5% (vol/vol) NP-40 in PBS for 2 h. Antibodies were diluted in 1.5% normal goat serum, 1% BSA and 0.25% NP-40 in PBS for 1 h. For c-Ret immunolabeling, an epitope demasking procedure was performed as described[24]. Nuclei were stained with DAPI. All sections were imaged using a Zeiss LSM 510 confocal microscope. Image analysis and stack assembly was performed off-line with ZEN 2009 light edition software (Zeiss) and Adobe Photoshop. For DRG cell counts, only neurons that contained visible nuclei were considered. To quantify the proportion of KCNQ4-positive lanceolate endings and Meissner corpuscles, these structures were identified by S100b staining and morphology. The built-in line-scan function of the LSM Zen 2008 software was used to measure peak fluorescence intensities of the plasma membrane. Peak plasma membrane and mean cytosolic fluorescence intensities were compared using Student's paired, two-tailed *t*-test. For quantification of lanceolate endings, the fluorescence intensity ratio of KCNQ4 and NF200 labeling was calculated and was compared between *Kcnq4*$^{+/+}$, *Kcnq4*$^{dn/+}$ and *Kcnq4*$^{dn/dn}$ mice using Student's *t*-test. Sections from at least three mice for each genotype were analyzed.

Electron microscopy. Mice were perfused with 4% PFA in 0.1 M phosphate buffer. Saphenous nerves were dissected and postfixed in 4% PFA, 2.5% (wt/vol) glutaraldehyde in 0.1 M phosphate buffer for 3 d. Following treatment with 1% (wt/vol) OsO_4 for 2 h, nerves were dehydrated in a graded ethanol series and propylene oxide and embedded in Poly/BedR 812 (Polysciences). Semi-thin sections were stained with toluidine blue. Ultrathin sections (70 nm) were contrasted with uranyl acetate and lead citrate and examined with a Zeiss 910 electron microscope. Digital images were taken with a CCD camera (Proscan) at an original magnification of 1,600×.

Antibodies. The following primary antibodies were used: rabbit anti-KCNQ4 (named rbKCNQ4KC)[10], 1:500; guinea pig anti-KCNQ4 (named gpKCNQ4A), 1:200 (raised against amino acids 2–12: AEAPPRRLGLG); rabbit anti-MafA, 1:10,000 (a kind gift from C. Birchmeier); mouse anti-NF200, 1:1,000 (Sigma); rabbit anti-NF200, 1:1,000 (Biozol); mouse anti-c-Ret, 1:20 (R&D); mouse anti-parvalbumin, 1:1,000 (Swant); rabbit anti-CK20, 1:25 (DAKO); rabbit anti-S100b, 1:400 (DAKO). Secondary antibodies were Alexa Fluor 488 goat anti–mouse IgG, Alexa Fluor 633 goat anti–mouse IgG, Alexa Fluor 555 goat anti–guinea pig IgG, Alexa Fluor 488 goat anti–rabbit IgG and Alexa Fluor 555 goat anti–rabbit IgG (Molecular Probes).

Retrograde labeling. Alexa Fluor 488–conjugated dextran (10–15 µl of 2.5% (wt/vol); relative molecular mass 3,000, anionic, Molecular Probes) was injected subcutaneously into the hairy skin and the plantar surface of hind paws. Mice were perfused 3 d after injection with PFA as described above and DRGs (vertebral levels L1–S3) were dissected for histochemical analysis.

***In vitro* skin nerve preparation.** The skin nerve preparation was used as previously described[28]. Adult mice were killed by placing them in a CO_2-filled chamber for 2–4 min followed by cervical dislocation. The saphenous nerve and the skin of the hind limb were dissected free and placed in a heated (32 °C) organ bath. The chamber was perfused with a synthetic interstitial fluid consisting of (in mM) NaCl, 123; KCl, 3.5; $MgSO_4$, 0.7; NaH_2PO_4, 1.7; $CaCl_2$, 2.0; sodium gluconate, 9.5; glucose, 5.5; sucrose, 7.5; and HEPES, 10 at a pH of 7.4. The skin was placed with the corium side up in the organ bath and the nerve was placed in an adjacent chamber for fiber teasing and single-unit recording. Single units were isolated with a mechanical search stimulus applied with a glass rod and classified by conduction velocity, von Frey hair thresholds and adaptation properties to suprathreshold stimuli as previously described[27]. Mechanical ramp-and-hold stimuli were applied with a computer-controlled nanomotor (Kleindiek Nanotechnik) and vibration stimuli were delivered with a piezo-actuator (Physik Instrumente PI) that was controlled by the built-in stimulator function of LabChart 7.1 (AD Instruments). The probe was a stainless steel metal rod with a flat circular contact area of 0.8 mm. To test the effect of linopirdine (Invitrogen), standardized suprathreshold displacement stimuli of 2 s duration were applied to the receptive field at regular intervals (interstimulus period, 58 s) for 12 min. Drugs were added to a stainless steel ring, which isolated receptive fields from the surrounding bath and prevented washout of the drug during the experiment.

The signal driving the movement of the mechanical stimulators and the raw electrophysiological data were recorded with a Powerlab 4/30 system and Labchart 7.1 software (AD Instruments) and spikes were discriminated off-line with the spike histogram extension of the software.

Patch-clamp recordings. HEK293 cells were transfected with KCNQ4 cDNA using Fugene HD transfection reagent (Roche) according to the manufacturers instructions and were used for patch-clamp recording 24 h after transfection. Whole-cell patch clamp recordings were made at 20–24 °C. Patch pipettes were pulled (Flaming-Brown puller, Sutter Instruments) from borosilicate glass capillaries (Hilgenberg), filled with a solution consisting of (in mM) KCl (110), NaCl (10), $MgCl_2$ (1), EGTA (1), HEPES (10) and ATP (2), adjusted to pH 7.3 with KOH, and had tip resistances of 6–8 MΩ. The bathing solution contained (in mM) NaCl (140), KCl (4), $CaCl_2$ (2), $MgCl_2$ (1), glucose (4), HEPES (10), adjusted to pH 7.4 with NaOH. Recordings were made using an EPC-10 amplifier (HEKA) in combination with Patchmaster and Fitmaster software (HEKA). Pipette and membrane capacitance were compensated using the auto function of Patchmaster, and series resistance was compensated by 70% to minimize voltage errors.

KCNQ4 mediated M-currents were activated with step depolarizations from −70 mV to −20 mV (2 s duration), and mechanosensitivity of KCNQ4 was tested by mechanically stimulating the cells during steady-state activation of the channels. Mechanical stimuli were applied with a fire-polished glass pipette (tip diameter, 2–3 µm) that was driven by a piezo-based Nanomotor micromanipulator (MM3A, Kleindiek Nanotechnik). The probe was positioned at an angle of 45° to the surface of the dish and moved with a velocity of 3.5 µm ms^{-1}.

Human psychophysics. The limits of spatial resolution in the fingertip were determined with a two-interval, forced-choice tactile grating orientation test that was performed with the Tactile Acuity Cube and TAG JVP Domes (Med-Core TAG) using a transformed-rule up and down trial design. Subjects had to detect whether a grating was pressed in longitudinal or transverse orientation against their fingers. Thresholds (79% probability) were calculated from the last 10 of 15 turning points.

doi:10.1038/nn.2985

Vibrotactile thresholds at different frequencies were determined with an ascending method-of-limits approach (**Fig. 7a**) using a custom-made device. Briefly, mechanical vibration stimuli of increasing amplitude (0–45 μm within 30 s) were delivered to the nail bed of the little finger with a piezo-actuator (Physik Instrumente PI) controlled by Powerlab 4/30 and LabChart 7.1 software. The probe was made of glass and had a flat circular contact area with a diameter of 5 mm. Subjects signaled the detection of vibratory stimuli by pressing a button. The little fingers of both hands were tested over a range of frequencies (5, 10, 20, 40, 80 and 160 Hz) and each frequency was tested in triplicate. To avoid acoustic perception of vibratory stimuli, white noise was played to the subjects through headphones during the testing. In some subjects, vibrotactile acuity at 125 Hz was also investigated using the CaseIV system (WR Medical Electronics), according to the manufacturers instructions. A two-interval, forced-choice, staircase trial design was used, and vibrotactile acuity was determined using the method of just noticeable differences.

Mouse tactile acuity test. Tactile acuity of mice was assessed using a two-choice preference test (grid test) as previously described[34]. Briefly, mice were placed in a completely dark arena that contained a grating cue (19, 38, 75 or 150 μm) embedded in the floor, and the mouse's activity was monitored for 30 min after an acclimatization period of 10 min using the Actimot system (TSE Systems). Each mouse was tested once per day, and the order of the tested grids was randomized for each mouse. To determine whether mice could reliably detect gratings of a certain size, the time spent on the grating cue was compared to the time spent on an equally sized control area (no cue) using Student's paired *t*-test (see **Supplementary Fig. 6**). Ratios were calculated for individual mice as (active time on grid)/(active time on control area).

Statistics. All data points represent means ± s.e.m. Statistical tests were performed using GraphPad Prism 5.0 software.